Microwave Spectrum of HOCH₂CD₂OH, and the Assignment of a Second Hydrogen-Bonded Conformation of Ethylene Glycol

Per-Erik Kristiansen,* K.-M. Marstokk and Harald Møllendal§

Department of Chemistry, The University of Oslo, P.O. Box 1033, Blindern, N-0315 Oslo 3, Norway

Kristiansen, P.-E., Marstokk, K.-M. and Møllendal, H., 1987. Microwave Spectrum of HOCH₂CD₂OH, and the Assignment of a Second Hydrogen-Bonded Conformation of Ethylene Glycol. – Acta Chem. Scand., Ser. A 41: 403–414.

Two heavy-atom *gauche* conformations of ethylene glycol, denoted *gGa* and *gGg*, may possess intramolecular hydrogen bonds. The microwave spectrum of *gGa* has previously been assigned. In this work, the *gGg* conformation is assigned and shown to be 1.4(4) kJ mol⁻¹ less stable than *gGa*. The O–C–C–O dihedral angle is 53.4(6)° in *gGa* and 53.9(6)° in *gGg*. Dipole moments and centrifugal distortion constants have also been determined for the two conformers.

The structure of ethylene glycol in the gas phase has interested chemists for years. Bastiansen[1] made an electron diffraction study of this compound as early as in 1949. He could only detect the heavy-atom *gauche* conformation, and no *anti* form. The stability of the *gauche* form was ascribed to intramolecular hydrogen bonding.[1] Very recently, Hedberg and coworkers[2] have made new electron diffraction experiments and studied the conformational composition of ethylene glycol at various temperatures. They could detect only the *gauche* form even at 460 °C. The heavy-atom *gauche* form thus has remarkable stability in the gas phase.

There are two possible heavy-atom *gauche* conformations possessing internal hydrogen bonds. They are denoted *gGa* and *gGg* and are depicted in Fig. 1. Further *gauche* conformations without hydrogen bonds are likely to have much higher energies and consequently a negligible population. Electron diffraction does not have sufficient resolution to differentiate between *gGa* and *gGg* because hydrogen atoms scatter electrons poorly. This method can tell us that the

heavy atoms are *gauche* but furnishes no information about the composition of *gGa* and *gGg*.

Structures predicted on the basis of *ab initio* calculations often mimic the gas phase structure quite well. Several computations using various basis sets have been made in recent years.[3–7] Small energy differences between *gGa* and *gGg* have been found in these calcuations. In the most recent calculation by van Alsenoy *et al.*,[7] the refinement was carried out, without any geometrical constraints, by the gradient method at the 4–21G level.

Low-temperature matrix studies often yield structural results which are similar to those found for the gaseous state. The results obtained for ethylene glycol by Günthard *et al.*[4,6] were interpreted in terms of only one hydrogen-bonded *gauche* conformation in the matrix, while Takeuchi and Tasumi[8] recently claimed that both *gGa* and *gGg* are present in substantial amounts in low-temperature argon matrices.

The high resolution of microwave (MW) spectroscopy makes it an ideal method for studying gaseous conformational equilibria, provided that the various conformers possess sizable dipole moments. The first MW study[9] revealed that ethylene glycol indeed has a strong spectrum. However, a straightforward rigid-rotor assignment of the MW spectrum of this compound could not be

---

*Present address: Styret for det industrielle rettsvern, Middelthuns gate 15b, Box 8160 Dep., N-0033 Oslo 1, Norway.
§To whom correspondence should be addressed.

Fig. 1. The two possible heavy-
atom *gauche* conformers
possessing intramolecular
hydrogen bonds. *gGg* differs from
gGa in that the O–H bond in the
proton-accepting hydroxyl group
is *gauche* to the C–C bond in
gGg and *anti* to this bond in *gGa*.
The *gGa* conformer is found to
be 1.4(4) kJ mol^{-1} more stable
than *gGg*.

gGa   gGg
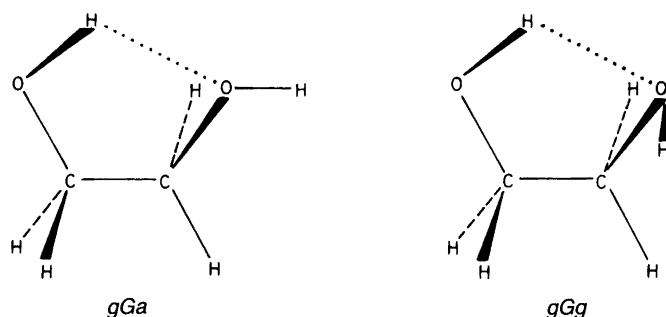
made because there are severe complications caused by extensive tunnelling of the two hydroxyl groups. No detailed assignments were therefore derived for this isotopic species.[9] This unusual tunnelling was presumed to arise because a reorientation of the hydroxyl group, which is a proton donor (or acceptor), into a situation where this group becomes a proton acceptor (or donor) leads to an identical molecule. Symmetrical double minimum potentials were thus presumed to exist[9] for each of the conformers *gGa* and *gGg*.

Tunnelling is substantially reduced in the dideuterated species DOCH$_2$CH$_2$OD which was later studied by Walder *et al.*[10] The single conformation found by these workers was undoubtedly the *gGa* form shown in Fig. 1. However, many absorption lines in the spectrum of DOCH$_2$CH$_2$OD remained unassigned,[10] and the coexistence of other stable forms such as *gGg* was considered to the quite likely.

Tunnelling in the MW spectrum of ethylene glycol is completely quenched if an asymmetric isotopic substitution is made, because symmetrical double minimum potential(s) will no longer exist. Ordinary rigid-rotor spectra, which are much less complex than the tunnelling spectra referred to above, are presumed for asymmetrically substituted isotopic species of this compound. This feature was exploited by Caminati and Corbelli.[11] They measured the MW spectrum of *O*-monodeuterated species in a mixture containing roughly 25 % of each of the four possible OH/OH, OH/OD, OD/OH and OD/OD isotopic species, and again assigned the *gGa* conformation, already identified by Walder *et al.*,[10] of two monodeuterated species which, as expected, displayed ordinary rigid-rotor MW spectra. The *gGg* conformation was searched for, but not

found in a very crowded, complex and not very intense spectrum. Two conformations with different heavy-atom arrangements have also been assigned for the closely related compound 1,2-propanediol.[12] The hydroxyl group conformations were similar to those of *gGa* in both these rotamers.[12] However, the spectrum of 1,2-propanediol is remarkably weak, which indicates that other conformers may coexist with the two already assigned.[12]

The conditions for finding additional rotamers of ethylene glycol other than *gGa* in the experiment reported by Caminati and Corbelli[11] were far from ideal; there were four different isotopic species, each present in a concentration of approximately 25 %. In addition, two of the spectra, viz. those of HOCH$_2$CH$_2$OH and DOCH$_2$CH$_2$OD, are both strong, complex and very crowded due to tunnelling. On top of this, the *gGg* conformation is present in substantial amounts in addition to the *gGa* form. Actually, the MW spectrum studied by the Italian workers[11] comprised no less than eight spectra superimposed on each other.

The situation is much more favourable for the unsymmetrical species HOCH$_2$CD$_2$OH studied in this work. Instead of eight superimposed spectra, there will now be four: two for *gGa* and two for *gGg*. The reason why there are two for each of these conformers is that the conformations of the HOCH$_2$- and HOCD$_2$-moieties are non-equivalent. For exactly 50 % of the molecules, the hydroxyl group of the HOCH$_2$-part is proton donor and the hydroxyl group oxygen atom of the HOCD$_2$-moiety is acceptor. The situation is of course reversed for the remaining 50 %. The two spectra observed for each of *gGa* and *gGg* are thus, in fact, the spectra of two isotopomers. Another great advantage is that tunnelling, which

results in much richer spectra than the ordinary rigid-rotor spectra, will be completely absent because $HOCH_2CD_2OH$ is unsymmetrical. Moreover, the fact that there are now four instead of eight spectra[11] also means that the intensity of each of them is twice as great as before.[11] The much simpler and stronger spectra displayed by $HOCH_2CD_2OH$, as compared with the experiment reported by Caminati and Corbelli,[10] should make a search for the *gGg* form a much more promising undertaking. This was the motivation for carrying out this work.

Experimental

Synthesis of $HOCH_2CD_2OH$. 10.0 g (0.13 mol) of glycolic acid was dissolved in 38 ml (0.53 mol) of absolute ethanol. 0.5 g of conc. hydrochloric acid was added and the mixture was heated under reflux for 4 h. The solution was then cooled and neutralized by addition of potassium carbonate. A fractional distillation at 52–56 °C/10 mmHg yielded 7.1 g (53 %) of glycolic acid ethyl ester. A mixture of 7 g (0.067 mol) of this ester and 11.5 g (0.13 mol) of 3,4-dihydro-2*H*-pyran was cooled to 0 °C. One drop of concentrated hydrochloric acid was now added and the solution was allowed to reach room temperature slowly (3 h). A few pellets of KOH were added and the solution was then distilled under reduced pressure. 11.2 g (89 %) of 2-tetrahydropyranyloxyglycolic acid ethyl ester was obtained at 60–65 °C/0.05 mmHg. 5.0 g (0.026 mol) of this compound dissolved in 15 ml of dry ether was added to 30 ml of dry ether containing 1.1 g (0.026 mol) of $LiAlD_4$ under a nitrogen atmosphere. The speed of this addition was regulated so that the ether boiled gently under reflux. After the addition was completed, the solution was stirred at room temperature for 1 h and heated under reflux for a further 1 h. The mixture was then cooled in a water/ice bath. Ice-cooled water was added dropwise until the evolution of hydrogen ceased. The precipitated aluminium salts were filtered off and washed with ether. The collected ether phase was dried with magnesium sulfate. The ether was distilled off, leaving 3.0 g (75 %) of 1,1-dideuterio-2-(2-tetrahydropyranyloxy)ethanol. 1.6 g (0.011 mol) of this compound was added dropwise to 25 ml of a 0.02 M solution of hydrochloric acid in methanol cooled to 0 °C. The mixture was allowed to reach room temperature slowly (2 h),

and then stirred overnight. The methanol and the 2-methoxytetrahydropyran thus formed (b.p. 125/760 mmHg) were removed by distilllation under reduced pressure. The crude product was purified by gas chromatography using a Porapak® Q column at 175 °C. The resulting $HOCH_2CD_2OH$ was identified by NMR and mass spectrometry [^{1}H NMR ($CDCl_3$) δ (ppm): 2.96 (s, 2 OH), 3.73 (s, CH_2); MS [m/e (r.i.)]: 64(11), 33(256), 31(271)].

Apparatus and experimental conditions. The spectrum was investigated in the 18.0–40.9 GHz region at room temperature, using a modified version of the spectrometer described in Ref. 13. Measurements were made with a vapour pressure of 1–2 Pa. The spectrum is rather dense because four species are present. The observed absorption lines were of moderate intensity. The strongest transitions had absolute peak intensities of roughly 3×10^{-7} cm^{-1}. These lines were the low-K_{-1} *a*-type $4 \leftarrow 3$ transitions of the two isotopomers of the *gGa* rotamer.

Results

Assignment of the gGa *conformation.* The *a*-axis dipole moment components of both isotopomers of this rotamer were presumed to be about as large as their counterparts in $DOCH_2CH_2OD$[10] and $HOCH_2CH_2OD$[11] (approximately 8×10^{-30} C m). The strong low-*J* *a*-type *R*-branch and the less intense *b*-type *Q*- and low-*J* *R*-branch spectra were readily assigned for both isotopic species. No *c*-type *Q*-branch lines were identified with certainty, presumably because the *c*-axis dipole moment component is quite small (see Dipole Moment section below). High-*J* *P*- and *R*-branch *b*-type transitions were too weak to be identified with certainty. The spectra of these two isotopomers are shown in Table 1, and the corresponding spectroscopic constants are listed in Table 2.

The first excited state of what is presumed to be the C–C torsional vibration was also assigned. The spectroscopic constants of this state are listed in Table 3. Relative intensity measurements performed largely as prescribed in Ref. 14 yielded 145(25) cm^{-1} for this vibration for both the two isotopomers. This is close to the values calculated for various isotopic species of ethylene glycol by Takeuchi and Tasumi.[8]

Table 1. Microwave spectrum of the *gGa* conformation of $HOCH_2CD_2OH$.

Isotopomer	$HOCH_2CD_2OH^a$		$HOCH_2\underline{CD_2OH}^a$	
Transition	Observed frequency[b]/MHz	Obs.–calc. frequency/MHz	Observed frequency[b]/MHz	Obs.–calc. frequency/MHz
$2_{0,2} \leftarrow 1_{0,1}$	19506.11	−0.01	19502.61	0.01
$2_{1,2} \leftarrow 1_{0,1}$	26795.87	−0.04	26858.90	−0.06
$2_{1,1} \leftarrow 1_{1,0}$	20515.04	0.03	20500.33	0.01
$2_{1,2} \leftarrow 1_{1,1}$	18648.82	0.10	18652.46	0.02
$3_{0,3} \leftarrow 2_{0,2}$	29072.94	−0.11	$-^c$	−
$3_{1,3} \leftarrow 2_{0,2}$	35217.26	0.08	35290.52	0.07
$2_{2,0} \leftarrow 2_{1,1}$	$-^c$	−	24693.14	0.01
$3_{1,2} \leftarrow 2_{1,1}$	30722.67	−0.08	30702.04	0.05
$3_{1,3} \leftarrow 2_{1,2}$	27927.45	0.06	27934.06	−0.03
$3_{2,1} \leftarrow 2_{2,0}$	29672.18	−0.03	29656.28	−0.02
$3_{2,2} \leftarrow 2_{2,1}$	29372.93	0.01	29364.62	0.00
$4_{0,4} \leftarrow 3_{0,3}$	38434.44	−0.05	38441.45	0.08
$3_{2,1} \leftarrow 3_{1,2}$	$-^c$	−	23647.36	−0.08
$4_{1,3} \leftarrow 3_{1,2}$	40865.30	−0.04	40840.23	−0.04
$4_{0,4} \leftarrow 3_{1,3}$	32290.35	−0.01	32223.27	−0.06
$4_{1,4} \leftarrow 3_{1,3}$	37156.57	0.11	37167.23	−0.03
$4_{2,3} \leftarrow 3_{2,2}$	39104.41	−0.02	39094.88	0.06
$4_{3,1} \leftarrow 3_{3,0}$	39327.62	0.04	39311.92	−0.03
$4_{3,2} \leftarrow 3_{3,1}$	$-^c$	−	39289.97	0.04
$4_{2,2} \leftarrow 4_{1,3}$	22433.49	−0.07	22611.93	−0.02
$4_{2,3} \leftarrow 4_{1,4}$	30634.45	−0.03	30749.48	0.09
$5_{1,4} \leftarrow 4_{2,3}$	$-^c$	−	29348.65	−0.05
$5_{2,3} \leftarrow 5_{1,4}$	21687.75	0.02	21851.11	0.00
$5_{2,4} \leftarrow 5_{1,5}$	$-^c$	−	33181.37	−0.12
$6_{1,5} \leftarrow 6_{0,6}$	21824.83	−0.04	21711.85	0.03
$6_{2,4} \leftarrow 6_{1,5}$	21490.59	0.04	21622.83	−0.06
$6_{2,5} \leftarrow 6_{1,6}$	36058.63	−0.04	$-^c$	−
$6_{3,3} \leftarrow 6_{2,4}$	$-^c$	−	40304.75	0.07
$7_{1,6} \leftarrow 7_{0,7}$	27055.77	0.07	26884.07	−0.02
$7_{2,5} \leftarrow 7_{1,6}$	22060.62	0.00	22144.38	0.06
$7_{2,6} \leftarrow 7_{1,7}$	$-^c$	−	39542.77	−0.06
$7_{3,4} \leftarrow 7_{2,5}$	38238.88	−0.07	38594.49	0.03
$8_{1,7} \leftarrow 8_{0,8}$	$-^c$	−	32810.15	0.05
$8_{2,6} \leftarrow 8_{1,7}$	23567.98	0.07	23584.80	−0.02
$8_{1,7} \leftarrow 8_{1,8}$	31932.37	−0.01	31664.98	0.03
$8_{3,5} \leftarrow 8_{2,6}$	36339.20	0.09	36701.13	−0.04
$9_{1,8} \leftarrow 9_{0,9}$	$-^c$	−	39252.66	0.04
$9_{2,7} \leftarrow 9_{1,8}$	26139.42	0.03	26071.88	0.07
$9_{3,6} \leftarrow 9_{2,7}$	34559.21	0.07	34905.45	−0.01
$10_{2,8} \leftarrow 10_{1,9}$	28847.38	0.01	29681.06	−0.01
$10_{3,7} \leftarrow 10_{2,8}$	33221.70	−0.03	33523.88	−0.07
$10_{2,8} \leftarrow 10_{2,9}$	23167.10	0.00	22778.24	0.00
$11_{2,9} \leftarrow 11_{1,10}$	34678.25	0.05	34407.11	0.02
$11_{3,8} \leftarrow 11_{2,9}$	32627.63	0.01	32855.43	0.03
$11_{2,9} \leftarrow 11_{2,10}$	$-^c$	−	29441.90	−0.08
$12_{2,10} \leftarrow 12_{1,11}$	40507.29	−0.04	40137.28	0.00
$12_{3,9} \leftarrow 12_{2,10}$	33020.17	−0.06	33144.55	0.07
$12_{2,10} \leftarrow 12_{2,11}$	$-^c$	−	36696.61	−0.08
$13_{3,10} \leftarrow 13_{2,11}$	34576.02	0.00	34570.76	0.02
$14_{3,11} \leftarrow 14_{2,12}$	37404.76	−0.03	37248.92	−0.06
$14_{3,11} \leftarrow 14_{3,12}$	24906.12	0.01	24273.74	−0.05
$15_{3,12} \leftarrow 15_{3,13}$	32174.32	0.00	31433.42	0.07

[a]Underlined hydrogen atom participates in the intramolecular hydrogen bond. [b]±0.10 MHz. [c]Not measured.

Table 2. Spectroscopic constants[a,b] for the ground vibrational state of the *gGa* conformation of HOCH$_2$CD$_2$OH.

Isotopomer	$\underline{\text{HOCH}_2\text{CD}_2\text{OH}}$[c]	$\text{HOCH}_2\text{CD}_2\text{O}\underline{\text{H}}$[c]
N.o.t.[d]	41	50
R.m.s.[e]/MHz	0.057	0.053
A_0/MHz	13509.256(14)	13562.6251(99)
B_0/MHz	5362.1116(72)	5356.1473(57)
C_0/MHz	4428.8576(70)	4432.1009(54)
Δ_J/kHz	5.30(26)	5.92(18)
Δ_{JK}/kHz	−24.44(18)	−21.78(13)
Δ_K/kHz	34.1(19)	35.5(13)
δ_J/kHz	1.8920(71)	1.9130(52)
δ_K/kHz	12.22(23)	11.12(15)

[a]*A*-reduction *I*[r]-representation. [b]Uncertainties represent one standard deviation. [c]Underlined hydrogen atom participates in the intramolecular hydrogen bond. [d]Number of transitions. [e]Root-mean-square deviation.

Table 3. Spectroscopic constants[a,b] for the first excited state of the C–C torsional mode of the *gGa* conformation of HOCH$_2$CD$_2$OH.

Isotopomer	$\underline{\text{HOCH}_2\text{CD}_2\text{OH}}$[c]	$\text{HOCH}_2\text{CD}_2\text{O}\underline{\text{H}}$[c]
N.o.t.[d]	29	21
R.m.s.[e]/MHz	0.100	0.104
A_v/MHz	13598.557(57)	13651.673(59)
B_v/MHz	5322.747(16)	5317.537(18)
C_v/MHz	4410.629(16)	4413.953(18)
Δ_J/kHz	5.92(56)	6.04(69)
Δ_{JK}/kHz	−25.37(57)	−32.17(66)
Δ_K/kHz	33.4(71)	35.5[f]
δ_J/kHz	1.922(25)	1.493(20)
δ_K/kHz	15.39(57)	21.96(68)

[a,b,c,d,e]Comments as for Table 2. [f]Preset ground-state value shown in Table 2.

Table 4. Stark coefficients[a] and dipole moment[a] of the *gGa* conformation of $\underline{\text{HOCH}_2\text{CD}_2\text{OH}}$.[b]

Transition		$\Delta\nu\ E^{-2}/10^{-6}$ MHz V^2 cm^{-2}	
		Obs.	Calc.
$3_{2,2} \leftarrow 2_{2,1}$	$M=0$	5.72(7)	5.74
$3_{1,2} \leftarrow 2_{1,1}$	$|M|=1$	−9.76(10)	−10.8
	$|M|=2$	−43.9(6)	−40.8
$3_{1,3} \leftarrow 2_{1,2}$	$M=0$	3.57(4)	3.56
	$|M|=1$	15.3(2)	15.1
$2_{1,1} \leftarrow 1_{1,0}$	$M=0$	16.5(2)	14.7

Dipole moment/10^{-30} C m

μ_a = 7.20(16) μ_b = 3.17(10) μ_c = 0[c] $\mu_{tot.}$ = 7.86(16)

[a]Uncertainties represent one standard deviation. [b]Underlined hydrogen atom participates in hydrogen bond. [c]Preset at zero; see text. 1 D = 3.33564×10^{-30} C m.

Table 5. Stark coefficients[a] and dipole moment[a] of the *gGa* conformation of $\text{HOCH}_2\text{CD}_2\text{O}\underline{\text{H}}$.[b]

Transition		$\Delta\nu\ E^{-2}/10^{-6}$ MHz V^2 cm^{-2}	
		Obs.	Calc.
$3_{2,2} \leftarrow 2_{2,1}$	$M=0$	6.40(7)	6.44
$3_{2,1} \leftarrow 2_{2,0}$	$M=0$	10.2(1)	10.9
$3_{1,2} \leftarrow 2_{1,1}$	$M=0$	0.305(3)	0.300
	$|M|=1$	−9.22(10)	−8.89
$3_{1,2} \leftarrow 2_{1,2}$	$M=0$	7.26(8)	7.39
$2_{1,1} \leftarrow 1_{1,0}$	$M=0$	14.1(2)	12.6

Dipole moment/10^{-30} C m

μ_a = 6.79(12) μ_b = 3.36(9) μ_c = 1.74(25) $\mu_{tot.}$ = 7.77(18)

[a,b]Comments as for Table 4.

Table 6. Microwave spectrum of the *gGg* conformation of $HOCH_2CD_2OH$.

Isotopomer	$HOCH_2CD_2OH$[a]		$HOCH_2CD_2OH$[a]	
Transition	Observed frequency[b]/MHz	Obs.–calc. frequency/MHz	Observed frequency[b]/MHz	Obs.–calc. frequency/MHz
$2_{1,1} \leftarrow 1_{0,1}$	29341.69	0.03	29360.85	0.07
$2_{1,2} \leftarrow 1_{0,1}$	–[c]	–	26670.28	0.11
$3_{0,3} \leftarrow 2_{0,2}$	–[c]	–	28876.70	0.03
$3_{1,2} \leftarrow 2_{0,2}$	40444.20	0.11	40448.64	0.05
$3_{1,2} \leftarrow 2_{1,1}$	–[c]	–	30454.22	0.11
$3_{1,3} \leftarrow 2_{1,2}$	27762.55	−0.08	27767.29	0.07
$3_{2,1} \leftarrow 2_{2,2}$	29446.63	−0.02	29432.89	0.03
$3_{2,2} \leftarrow 2_{2,1}$	29162.90	−0.03	29154.91	−0.11
$4_{0,4} \leftarrow 3_{0,3}$	–[c]	–	38195.18	−0.07
$4_{1,3} \leftarrow 3_{1,2}$	40537.05	0.01	40514.66	−0.06
$4_{0,4} \leftarrow 3_{1,3}$	32049.82	0.11	32000.80	−0.04
$4_{1,4} \leftarrow 3_{1,3}$	36940.73	−0.08	36948.56	−0.03
$4_{2,2} \leftarrow 3_{2,1}$	–[c]	–	39495.22	−0.03
$4_{2,3} \leftarrow 3_{2,2}$	38827.51	−0.05	38818.25	−0.10
$4_{2,2} \leftarrow 4_{1,3}$	22298.81	−0.05	22420.67	0.07
$4_{2,3} \leftarrow 4_{1,3}$	21252.64	0.00	21.395.67	−0.01
$4_{2,2} \leftarrow 4_{1,4}$	31318.63	−0.05	31364.23	−0.01
$4_{2,3} \leftarrow 4_{1,4}$	–[c]	–	30339.32	0.00
$5_{2,3} \leftarrow 5_{1,4}$	21545.17	−0.07	21656.58	0.01
$5_{2,4} \leftarrow 5_{1,4}$	19185.80	−0.04	–[c]	–
$5_{2,4} \leftarrow 5_{1,5}$	32652.98	−0.07	32698.31	−0.12
$6_{0,6} \leftarrow 5_{1,4}$	39061.38	0.00	–[c]	–
$6_{1,5} \leftarrow 5_{2,3}$	–[c]	–	38680.22	0.07
$6_{1,5} \leftarrow 6_{0,6}$	21297.76	−0.08	21196.53	−0.06
$6_{2,4} \leftarrow 6_{1,5}$	21308.76	−0.06	21397.16	−0.08
$6_{2,5} \leftarrow 6_{1,6}$	–[c]	–	35546.33	−0.07
$6_{3,3} \leftarrow 6_{2,4}$	39753.25	−0.03	–[c]	–
$6_{3,4} \leftarrow 6_{2,4}$	39461.05	−0.01	39699.89	−0.05
$7_{1,6} \leftarrow 7_{0,7}$	26358.75	0.02	26208.42	−0.07
$7_{2,5} \leftarrow 7_{1,6}$	21802.26	−0.06	21853.91	−0.03
$7_{3,4} \leftarrow 7_{2,5}$	38080.57	0.10	38326.58	0.06
$7_{3,5} \leftarrow 7_{2,5}$	37364.65	−0.11	37633.91	−0.02
$8_{1,7} \leftarrow 8_{0,8}$	32162.40	−0.03	31965.93	0.00
$8_{3,5} \leftarrow 8_{2,6}$	36222.75	0.09	36476.30	0.11
$8_{3,6} \leftarrow 8_{2,6}$	–[c]	–	34998.40	−0.05
$9_{1,8} \leftarrow 9_{0,9}$	38478.78	0.04	38244.55	−0.02
$9_{2,7} \leftarrow 9_{1,8}$	25603.22	−0.03	25537.95	−0.02
$9_{3,6} \leftarrow 9_{2,7}$	34452.13	0.06	34696.52	−0.10
$9_{3,7} \leftarrow 9_{2,7}$	31537.33	0.07	–[c]	–
$10_{2,8} \leftarrow 10_{1,9}$	29111.85	0.00	28968.96	0.09
$10_{3,7} \leftarrow 10_{2,8}$	33077.47	0.09	33291.32	−0.08
$10_{3,8} \leftarrow 10_{2,8}$	27997.04	0.02	28357.52	0.07
$11_{2,9} \leftarrow 11_{1,10}$	33715.61	0.10	33488.34	−0.14
$11_{3,8} \leftarrow 11_{2,9}$	32391.49	0.12	32551.32	0.03
$11_{3,9} \leftarrow 11_{2,9}$	24208.37	0.03	24589.18	0.11
$12_{2,10} \leftarrow 12_{1,11}$	39308.28	0.02	38999.88	0.18
$12_{3,9} \leftarrow 12_{2,10}$	32634.98	0.01	32717.86	0.08
$12_{3,10} \leftarrow 12_{2,10}$	20323.28	0.00	20713.75	0.10

Table 6 (contd).

Isotopomer	$\underline{HO}CH_2CD_2OH^a$		$HOCH_2CD_2\underline{OH}^a$	
Transition	Observed frequency^b/MHz	Obs.–calc. frequency/MHz	Observed frequency^b/MHz	Obs.–calc. frequency/MHz
$13_{1,10} \leftarrow 13_{2,11}$	33985.83	0.05	33970.46	−0.07
$14_{3,11} \leftarrow 14_{2,12}$	36558.56	0.01	$-^c$	−
$14_{4,11} \leftarrow 14_{3,11}$	40686.91	−0.09	$-^c$	−
$15_{3,12} \leftarrow 15_{2,13}$	40396.81	−0.13	$-^c$	−
$15_{4,12} \leftarrow 15_{3,12}$	35863.30	−0.08	36493.99	0.02
$16_{4,13} \leftarrow 16_{3,13}$	30835.23	0.01	31488.21	−0.07
$17_{4,14} \leftarrow 17_{3,14}$	25792.74	−0.05	26448.38	−0.09
$18_{4,15} \leftarrow 18_{3,15}$	20936.05	0.08	21570.95	−0.08
$21_{5,17} \leftarrow 21_{4,17}$	36981.74	−0.03	37962.34	−0.06
$22_{5,18} \leftarrow 22_{4,18}$	30897.73	0.12	31869.40	0.04
$23_{5,19} \leftarrow 23_{4,19}$	$-^c$	−	26027.62	0.07
$24_{5,20} \leftarrow 24_{4,20}$	19791.38	−0.09	20646.90	0.02

^{a,b,c}Comments as for Table 1.

Dipole moment. The principal axes components of the dipole moment must be known in order to determine the energy difference between the two rotamers of ethylene glycol. A determination of the dipole moments was therefore carried out using standard procedure.[15] The results are given in Tables 4 and 5. The *c*-axis component of the species of Table 4 was found to be imaginary. This component was therefore preset to a value of zero C m in the final fit. The total dipole moments of these two isotopomers of *gGa* are quite similar to those found for $DOCH_2CH_2OD^{10}$ [8.04(50) 10^{-30} C m] and one of the $DOCH_2CH_2OH^{11}$ species [7.60(40) 10^{-30} C m], as expected.

The principal axes dipole moment components for the isotopomer of Table 4 were calculated using the bond-moment method,[16] employing the plausible structural data of Table 10. It was assumed that both hydroxyl groups were completely staggered. The results were: $\mu_a = 7.34$, $\mu_b = 3.17$ and $\mu_c = 0.27$ (in units of 10^{-30} C m). These values are very close to those recorded in Table 4. Likewise, $\mu_a = 7.60$, $\mu_b = 2.53$ and $\mu_c = 0.43$ (in units of 10^{-30} C m) were computed[16] for the isotopomer of Table 5, in good agreement with the values shown in that table.

The most recent dipole moment computations by the *ab initio* method[7] gives a value which is too large by about 45%.

Assignment of the gGg *conformation.* After the above assignments had been made, several lines distributed throughout the spectrum remained unassigned. The strongest of these were roughly 1/3 as strong as those for the ground state *a*-type transitions of the predominant *gGa* conformation. The possibility that they all were unassigned high-*J* transitions of the ground state, or belonging to other vibrationally excited states of this form was considered to be most unlikely. The possibility that they might belong to any heavy-atom *anti* conformation was thought to be out of the question in view of the new electron-diffraction findings.[2] Their modulation patterns suggested that they had to be *Q*-branch transitions of the *b*- or *c*-type.

The bond-moment method[16] was used to predict the principal axes dipole moment components assuming the hydroxyl group hydrogen atoms of *gGg* to be located in exactly staggered positions. Sizable values were predicted for all three principal axes dipole moment components. The prominent *b*- and *c*-type *Q*-branch lines were then searched for and identified after some effort. The much weaker low-*J* *R*-branch transitions of *a*-, *b*- and *c*-type were found next. The spectra of the two isotopomers of *gGg* are listed in Table 6 and the spectroscopic constants derived from these transitions are listed in Table 7.

The high-*J* *c*-type *Q*-branch lines of both isotopomers of the *gGg* conformation were found to display noteworthy behaviour. No problems were encountered in fitting these lines using the *A*-

Table 7. Spectroscopic constants[a,b] for the ground vibrational state of the *gGg* conformation of $HOCH_2CD_2OH$.

Isotopomer	$HOCH_2CD_2OH^c$	$\underline{HOCH_2CD_2OH}^c$
N.o.t.[d]	50	54
R.m.s.[e]/MHz	0.072	0.080
A_0/MHz	13403.4288(97)	13438.063(10)
B_0/MHz	5312.8086(63)	5307.6247(60)
C_0/MHz	4408.1483(64)	4410.6722(60)
Δ_J/kHz	4.96(15)	3.50(15)
Δ_{JK}/kHz	−24.61(11)	−21.06(13)
Δ_K/kHz	49.7(11)	44.6(13)
δ_J/kHz	1.8710(38)	1.9061(43)
δ_K/kHz	11.14(15)	8.83(19)

[a,b,c,d,e]Comments as for Table 2.

reduction I^r-representation[17] with only quartic centrifugal distortion terms up to the $K_{-1} = 5 \leftarrow 4$ transitions, as shown in Table 6. However, the next series of $K_{-1} = 6 \leftarrow 5$ were perturbed for both isotopomers and could not be fitted well to this Hamiltonian even if sextic centrifugal distortion terms were included. The perturbations were not large, amounting to a few MHz. Higher Q-branch transitions also appeared to be perturbed by a few MHz.

The high-J R-branch lines of the b- and c-type were predicted to coalesce. Relatively high intensities result because of this coalescence and because both the b- and c-axis dipole moment components are sizeable (see Dipole Moment section below). In addition, the fact that μ_a is non-zero leads to a very rapid and characteristic Stark effect for such lines. The frequencies of these coalescing transitions could be rather well predicted. It is felt that several such lines have been identified. However, they could not be fitted well to the usual Watson Hamiltonian,[17] presumably as a result of perturbations. The perturbations thus observed both for the high-J Q- and R-branch transitions may arise from the low barriers between the *gGa* and/or *gGg* conformations.

Dipole moment. The low-J transitions of the *gGg* rotamer were all so weak that they could not be employed for quantitative Stark effect measurements. The stronger medium-J Q-branch transitions had to be used. Neither the resolution of the Stark components of these transitions nor their intensities were as good as one would wish. The Stark components have therefore been assigned larger standard deviations than usual (see Tables 8 and 9). The results obtained following the normal procedure[15] are shown in Tables 8 and 9. It is seen that μ_a is quite similar for both isotopomers, while both μ_b and μ_c deviate from one another more than expected. The uncertainties of these components are also quite large. This has to do with the rather poor quality of the data at hand. However, it is reassuring to see that the total dipole moment is quite similar for both isotopomers.

The dipole moment components were computed using the bond-moment method,[16] assum-

Table 8. Stark coefficients[a] and dipole moment[a] of the *gGg* conformation of $\underline{HOCH_2CD_2OH}$.[b]

Transition		$\Delta v\ E^{-2}/10^{-5}$ MHz V^2 cm^{-2}	
		Obs.	Calc.
$9_{3,7} \leftarrow 9_{2,7}$	$\lvert M \rvert = 9$	−0.634(12)	−0.659
$7_{3,5} \leftarrow 7_{2,5}$	$\lvert M \rvert = 7$	−9.42(20)	−8.59
$9_{2,7} \leftarrow 9_{1,8}$	$\lvert M \rvert = 8$	2.36(5)	2.63
$6_{2,4} \leftarrow 6_{1,5}$	$\lvert M \rvert = 6$	2.28(4)	2.17
$11_{3,8} \leftarrow 11_{2,9}$	$\lvert M \rvert = 11$	1.14(2)	1.11
$8_{3,5} \leftarrow 8_{2,6}$	$\lvert M \rvert = 8$	3.18(6)	3.19
Dipole moment/10^{-30} C m			
$\mu_a = 4.44(13)$	$\mu_b = 3.58(60)$	$\mu_c = 5.93(23)$	$\mu_{tot.} = 8.23(45)$

[a,b]Comments as for Table 4.

ing the positions of the hydroxyl groups to be exactly staggered, as in the above-mentioned case of the *gGa* conformation. For the isotopomer of Table 8, the following results were computed: $\mu_a = 2.67$, $\mu_b = 1.90$ and $\mu_c = 7.27$ (in units of 10^{-30} C m). This is the only fair agreement with the experimental results shown in the same table. For the isotopomer of Table 9, the predicted[16] values were $\mu_a = 2.47$, $\mu_b = 2.60$ and $\mu_c = 7.10$ (with the same units as above). Again, the agreement between computed and experimental values is only fair (see Table 9). However, the total dipole moments of both these isotopomers are in quite good agreement with the experimental results.

The dipole moment found by *ab initio* calculations[7] is also in this case too large by roughly 40 %.

Energy difference. The internal energy difference (ΔE°) between the gGg and *gGa* conformations was determined from intensity comparisons in the limit of no power saturation.[18] Two series of comparisons were made. In the first series of measurements, the *gGg* and *gGa* rotamers both having the proton-donating hydroxyl group attached to the $-CD_2-$ group (and the proton-accepting hydroxyl group attached to the $-CH_2-$ group) were compared. In the second series, the reverse situation (hydroxyl group of $HOCH_2-$ moiety as donor) was employed. In both these cases the energy differences were found to be the same within experimental accuracy. A value of $\Delta E^\circ = 1.4$ kJ mol^{-1} was found, with *gGa* being

the more stable. A liberal estimate of one standard deviation is ± 0.4 kJ mol^{-1}. The most recent *ab initio* value[7] for this energy difference is 3.7 kJ mol^{-1}, which is outside the experimental error limit.

Structure. 15 rotational constants for five deuterated species of the *gGa* conformation of ethylene glycol are now available. Three of these species were those studied previously,[10,11] and the remaining two are those found in this work (Table 2). In addition, 6 rotational constants have been determined for the *gGg* conformation (Table 7). Attempts to fit several of the structural parameters to the rotational constants were made using the least-squares method, but high correlations and standard deviations were encountered, presumably because data for ^{13}C and ^{18}O substituted species are not yet available. It was therefore decided to fit only the O–C–C–O dihedral angle of each conformation, keeping the remaining structural parameters fixed at the values shown in Table 10. These parameters have been selected from recent accurate studies of closely related compounds.

One comment is in order regarding the C–C–O angles of Table 10. When the O–H bond is *anti* to the C–C bond this angle is assumed to have a value of 107.8°, which was actually found for *anti* ethanol.[19] This angle increases by 4–5° (see Ref. 20 for a discussion) when the O–H bond is *gauche* to the C–C bond rather than *anti*. In this work, a value of 112.0° was assumed for this particular angle. In the *gGa* conformation, the C–C–O an-

Table 9. Stark coefficients[a] and dipole moment[a] of the *gGg* conformation of $HOCH_2CD_2O\underline{H}$.[b]

Transition		Δν E^{-2}/10^{-5} MHz V^2 cm^{-2}	
		Obs.	Calc.
$9_{2,8} \leftarrow 9_{1,8}$	$\lvert M \rvert = 9$	2.32(5)	2.12
$7_{2,5} \leftarrow 7_{1,6}$	$\lvert M \rvert = 7$	1.85(4)	2.02
$8_{1,7} \leftarrow 8_{0,8}$	$\lvert M \rvert = 8$	17.3(4)	18.1
$11_{3,8} \leftarrow 11_{2,9}$	$\lvert M \rvert = 11$	0.963(20)	1.04
$13_{3,10} \leftarrow 13_{2,11}$	$\lvert M \rvert = 13$	1.29(2)	1.20
$8_{3,5} \leftarrow 8_{2,6}$	$\lvert M \rvert = 8$	2.99(6)	2.92

Dipole moment/10^{-30} C m

$\mu_a = 4.45(21)$	$\mu_b = 5.31(29)$	$\mu_c = 3.79(20)$	$\mu_{tot.} = 7.90(32)$

^{a,b}Comments as for Table 4.

gle of the proton-donating oxygen atom was thus held fixed at 107.8° while the C–C–O angle of the proton-accepting oxygen was kept fixed at 112.0°. In the gGg rotamer, both C–C–O angles were fixed at 112.0°. The remaining structural parameters (with the exception of the O–C–C–O dihedral angle) were assumed to have the same values for the two conformations and were held fixed at the values shown in Table 10.

There are several reasons why the O–C–C–O dihedral angles of the two conformations gGa and gGg were selected for fitting: The rotational constants are all very sensitive to variation of this parameter. It is also difficult to estimate accurate values for the O–C–C–O dihedral angle in advance. Moreover, more than any other structural parameter this angle may reflect the unusually strong interaction between the two hydroxyl groups which must be responsible for the unique stability of the heavy-atom *gauche* form, as shown anew in the very recent electron diffraction study.[2]

The results of the least-squares fits are shown in Tables 10 and 11. The O–C–C–O dihedral angle of gGa was determined to be 53.64(40)° from *syn*, nearly the same as for gGg, where 53.94(24)° was found. The quoted standard deviations do not reflect the systematic uncertainties in the plausible structural parameters which were not fitted. An estimate of this source of error led us to increase the standard deviations somewhat. As final values, the O–C–C–O angles are taken as 53.6(6)° for gGa, and 53.9(6)° for gGg. The values computed by van Alsenoy et al.[7] were 57.29° for gGa and 53.37° for gGg, respectively.

Discussion

The recent electron diffraction work by Hedberg et al.[2] indicates that the heavy-atom *gauche* conformations both must be at least 12 kJ mol⁻¹ more stable than any of the heavy-atom *anti* conformations. The lowest energy difference calculated by *ab initio*[7] methods was about 7 kJ mol⁻¹. The fact that the O–C–C–O dihedral angles of both gGa and gGg are roughly 6° less than completely staggered also indicates that a strong interaction between the two hydroxyl groups exists in this molecule. The internal hydrogen bonds alone cannot account for this stability. As shown in Table 10, the H···O distances of the hydrogen bonds of gGa and gGg are only slightly shorter

Table 10. Plausible molecular structure[a] [bond lengths (pm), angles (°)] of the gGa and gGg conformations of ethylene glycol.

Structural parameters kept fixed

C–O	142.0	∠CCO	107.8[b], or 112.0[c]
C–C	153.0	∠COH	104.5
O–H	95.0	∠CCH	109.47
C–H	109.3	∠HOCC	0.0[d], or 120.0[d]

Fitted

∠OCCO	53.64(40)[e] from *syn* for gGa
∠OCCO	53.94(24)[e] from *syn* for gGg

Hydrogen bond parameters

Conformation:	gGa	gGg
H···O[f]	236.0	245.7
O···O[g]	277.1	288.5
∠O–H···O	105.6	105.1
∠O–H,O–H[h]	72.5	72.4

Sum of van der Waals radii[i]

H···O	260
O···O	280

[a]See text. [b]When O–H bond is *anti* to the C–C bond; see text. [c]When the O–H bond is *gauche* to the C–C bond; see text. [d]H–O–C–C dihedral angle. 0° indicates that the O–H bond is *anti* to the C–C bond, whereas 120° indicates that the O–H bond is *gauche* to the C–C bond. [e]Uncertainties represent one standard deviation obtained from the fit shown in Table 11. See also text for a discussion of the uncertainties in the O–C–C–O dihedral angles of the two conformers. [f]Distance between hydrogen and oxygen atoms involved in hydrogen bonding. [g]Nonbonded distance between the oxygen atoms. [h]Angle between the two hydroxyl groups. [i]Taken from Ref. 21.

than the sum of the van der Waals radii of hydrogen and oxygen.[21] Dipole–dipole interaction between the two O–H bonds in each of these rotamers must also be rather weak, as can be inferred from Table 10. The O–H stretching vibrational frequencies are also typical for a weak intramolecular hydrogen bond.[8]

In order to explain the electron diffraction findings, an effect in addition to the internal hydrogen bonding must be operative. This so-called *gauche effect*[22] is important for electronegative substituents. In ethylene glycol it must augment the hydrogen bonding and be of considerable

Table 11. Least-squares fit of the O–C–C–O dihedral angle[a] to the rotational constants.

Species	Observed rot. const.			Obs.-calc. rot. const.		
	A/MHz	*B*/MHz	*C*/MHz	Δ*A*/MHz	Δ*B*/MHz	Δ*C*/MHz
gGa conformation						
DOCH$_2$CH$_2$OD[b]	14394.6	5276.3	4323.5	−87.7	−31.1	34.0
DOCH$_2$CH$_2$OH[c,d]	14620.3	5548.5	4517.9	9.2	−50.9	30.3
ḎOCH$_2$CH$_2$OH[c,d]	15127.0	5311.1	4412.2	−55.6	−48.8	31.0
HOCH$_2$CD$_2$OH̱[d,e]	13562.6	5356.1	4432.1	35.1	−60.9	32.6
H̱OCH$_2$CD$_2$OH̱[d,e]	13509.3	5362.1	4428.9	−0.2	−55.2	33.4
gGg conformation						
HOCH$_2$CD$_2$OH̱[d,e]	13438.1	5307.6	4410.7	11.2	−5.2	23.0
H̱OCH$_2$CD$_2$OH̱[d,e]	13403.4	5312.8	4408.1	−9.7	−1.1	23.0

O–C–C–O dihedral angles

gGa conformation   53.64(40)° from *syn*[f]
gGg conformation   53.94(24)° from *syn*[f]

[a]Using the plausible structural parameters shown in Table 10; see text. [b]Taken from Ref. 10. [c]Taken from Ref. 11. [d]Underlined hydrogen atom participates in hydrogen bond. [e]This work. [f]Uncertainties represent one standard deviation obtained in the least-squares fit. See text for discussion of errors.

magnitude. In fact, the *gauche effect* is believed to be more important than hydrogen bonding.

The reason why the *gGa* conformation is preferred to the *gGg* form by 1.4(4) kJ mol^{-1} is not obvious. Perhaps the fact that there are two *gauche* arrangements around the C–O bonds in *gGg* and only one such arrangement in gGa is part of the explanation. It is known[23] that the *gauche* conformer of ethanol is less stable than the *anti* by as much as 2.9(2) kJ mol^{-1}. A similar finding has been made for 3-hydroxypropano-nitrile.[20] In this molecule the *Anti II* rotamer is less stable than *Anti I* by 4.7(20) kJ mol^{-1}. The difference between these two conformations[20] involves just an *anti* to *gauche* rotation around a C–O bond, exactly as in ethanol[23] and in the present case of ethylene glycol.

References

1. Bastiansen, O. *Acta Chem. Scand. 3* (1949) 415.
2. Kazerouni, M. R., Barkowski, S. L., Hedberg, L. and Hedberg, K. *Proceedings of the Eleventh Austin Symposium on Molecular Structure* (1986), Austin 1986, p. 33.
3. Radom, L., Lathan, W. A., Hehre, W. J. and Pople, J. *J. Am. Chem. Soc. 95* (1973) 693.
4. Ha, T.-K., Frei, H., Meyer, R. and Günthard, H. H. *Theor. Chim. Acta 34* (1974) 277.
5. Almlöf, J. and Stymne, H. *Chem. Phys. Lett. 33* (1975) 118.
6. Frei, H., Ha, T.-K., Meyer, R. and Günthard, H. H. *Chem. Phys. 25* (1977) 271.
7. van Alsenoy, C., van den Enden, L. and Schäfer, L. *J. Mol. Struct. (Theochem) 108* (1984) 108.
8. Takeuchi, H. and Tasumi, M. *Chem. Phys. 77* (1983) 21.
9. Marstokk, K.-M. and Møllendal, H. *J. Mol. Struct. 22* (1974) 301.
10. Walder, E., Bauder, A. and Günthard, H. H. *Chem. Phys. 51* (1980) 223.
11. Caminati, W. and Corbelli, G. *J. Mol. Spectrosc. 90* (1981) 572.
12. Caminati, W. *J. Mol. Spectrosc. 86* (1981) 193.
13. Marstokk, K.-M. and Møllendal, H. *J. Mol. Struct. 5* (1970) 205.

14. Esbitt, A. S. and Wilson, E. B. *Rev. Sci. Instrum.* 28 (1963) 901.
15. Marstokk, K.-M. and Møllendal, H. *Acta Chem. Scand., Ser. A 34* (1980) 15.
16. Smyth, C. P. *Dielectric Structure and Behavior,* McGraw-Hill, New York 1955, p. 244.
17. Gordy, W. and Cook, R. L. *Microwave Molecular Spectra,* Wiley, New York 1984, p. 324.
18. Townes, C. H. and Schawlow, A. L. *Microwave Spectroscopy,* McGraw-Hill, New York 1955, p. 372.
19. Culot, J. P. *Proceedings of the Fourth Austin Symposium on Gas Phase Molecular Structure,* Austin 1972, Paper T8.
20. Marstokk, K.-M. and Møllendal, H. *Acta Chem. Scand., Ser. A 39* (1985) 15.
21. Pauling, L. *The Nature of the Chemical Bond,* 3rd ed., Cornell University Press, New York 1960, p. 260.
22. Wolfe, S. *Acc. Chem. Res. 5* (1972) 102.
23. Fang, H. L. and Swofford, R. L. *Chem. Phys. Lett. 105* (1984) 5.